Practical Responses to Climate Change
ENGINEERS AUSTRALIA CONVENTION 2014
25-27 NOV MELBOURNE

Conceptual Design of an Unmanned Aircraft Laser System for Aviation Pollution Measurements

Alessandro Gardi[1,†], *Roberto Sabatini*[1,‡], *Graham Wild*[1]

[1]*School of Aerospace, Mechanical and Manufacturing Engineering, RMIT University, Melbourne, VIC 3000, Australia*

Abstract

This paper presents the recent research activities aimed at developing a flexible and low-cost measurement system for the determination of aviation-related pollutant concentrations in dense air traffic areas. The proposed bistatic Light Detection and Ranging (LIDAR) system includes an airborne component and a ground-based component. The airborne component consists of a tuneable laser emitter installed on an Unmanned Aircraft (UA) and the ground-based component is constituted by a target surface calibrated for reflectance and a rail-mounted camera calibrated for radiance. The system performs Differential Absorption LIDAR (DIAL) measurements. The specific implementation for the measurement of CO_2 in the aerodrome traffic zone of a major airport is studied in this paper. The analytical and empirical models to directly estimate the extinction coefficients are also presented and uncertainty analysis is performed for a preliminary validation of the bistatic DIAL system. The relevant opportunities and challenges, and the viability of the system in the intended operational domains are also discussed. The presented numerical results show satisfactory performances in term of accuracy and precision even in degraded meteorological conditions, which are comparable to the more complex and relatively costly techniques currently available.

Keywords: Aircraft Emissions, Differential Absorption, DIAL, LIDAR, Pollutant Measurement, Sustainable Aviation.

1. Introduction

The steady growth of air transport at the global scale in the last decades has prompted social, political and scientific reactions to address its largely unsustainable evolution. Although aviation is currently producing less than 3% of the overall man-made CO_2 emissions, the global community is working to reduce the relative level of emissions as growth in air transport is forecast to increase such emissions by 50% over current levels by 2050 (Janić, 2007). Major research and development programmes were therefore launched, including Clean Sky, NextGen, SESAR, Greener by Design, Environmentally Responsible Aviation, and are now delivering their preliminary outcomes to the industry and to the political decision-makers. The R&D activities are focusing on several concepts and technologies to reduce environmental impacts of flight operations, as well as in manufacturing, logistics, assembly, and disposal chains. Fossil fuels are particularly addressed since at present they represent by far the largest energy source for aircraft propulsion. The combustion of fossil fuels originates a number of noxious compounds as well as greenhouse gases, of which carbon dioxide (CO_2) is the principal representative, being the largest component of exhaust emissions. As a reference, each ton of typical Jet-A1 fuel can develops up to 3.15 tons of CO_2, therefore the impact of each single commercial flight, typically consuming several tons of fuel, is substantial. The legislation currently in place for noise pollution control and charging is gradually being extended to CO_2 and it is envisaged that will similarly involve other polluting gases as well in the future. Therefore, high air traffic density areas will likely be actively monitored in terms of pollutant emissions. This fact, together with the ever rising scientific demand for more precise measurements of the investigated pollutants, are supporting research activities for the design of new sensor technologies and innovative measurement systems. The new systems should feature either: greater operational flexibility, better sensitivity, accuracy, precision, reliability, greater spectral/spatial/temporal resolutions, and reduced weight/volume/costs. The scientific research is interested, in particular, in the spatial and temporal variation of macroscopic observables, and on the microphysical and chemical properties of atmospheric constituents and pollutants, including molecular, aerosol and particulate species (Rodgers, 2000; Sabatini & Richardson, 2010a; Sabatini, Richardson, et al., 2012). For all the mentioned reasons, it is evident that an accurate characterisation of CO_2 concentrations in space and time around a variety of aircraft operations is particularly important.

[†] Lead and Presenting Author: alessandro.gardi@rmit.edu.au

[‡] Corresponding Author - roberto.sabatini@rmit.edu.au

2. Pollutant measurement techniques

Ignoring dedicated test-bench installations, the adopted measurement strategies for aircraft pollutant emission figures are based on the following techniques (Gardi, Sabatini & Wild, 2014):

- Air quality sampling stations: they are located in the vicinity of larger airports and are the main source for their average pollution figures. All pollutant emissions from man-made and biogenic activities in the surroundings of the air quality station are detected and cumulatively participate to the measure. Their measurement is also substantially affected by aerodynamic effects as advection and diffusion of pollutants and is therefore noticeably averaged in time and space. For all these reasons these measurements are natively incapable of discerning a single aircraft, let alone a particular phase of its flight.
- On-board thermomechanical sensors: they are installed within the aircraft engines and more generally on board aircraft, allowing an indirect estimation of pollutant emissions based on certain models and assumptions. Most commonly installed sensors are typically measuring Fuel Flow (FF), Turbine Entry Temperature (TET), Exhaust Gas Temperature (EGT), Engine Pressure Ratio (EPR), engine rotation speed (N_1, N_2, N_F...) and acoustic vibrations. The indirect estimation of pollutant emissions is analytically or heuristically derived from these thermodynamic and mechanical measurements, and is based on nominal conditions. Significantly off-design or degraded conditions of engine, fuel chemical composition, fuel transport or fuel storage conditions may violate key assumptions and hence affect the validity of such indirect measurements.
- Remote sensing: typically performed by satellites, aircraft and balloons. The most widely used techniques for remote atmospheric sounding are based on absorption spectroscopy performed by passive electro-optic systems and on differential absorption measurements performed by LIDAR. A number of airborne and spaceborne laser systems have been adopted for large-scale CO_2 column density measurement campaigns (Abshire et al., 2010; Allan et al., 2008; Amediek et al., 2009; Krainak et al.; Riris et al., 2007; Sabatini & Richardson, 2008). Remote sensing from satellites and conventional aircraft are nonetheless affected by substantial costs and a rather limited flexibility in terms of space and time patterns and resolutions of the measures.

All these limitations support the study, design and development of innovative direct concentration measurement techniques. The advent of powerful LIDAR systems with low weight and packaged in relatively small casings, allowed them to be well suited for measuring the column densities of various important molecular species, including carbon oxides (CO_X), nitrogen oxides (NO_X), sulphur dioxides (SO_X), O_2 and ozone (O_3), both locally and over extended geographic areas (Müller et al., 2000; Veselovskii et al., 2004). The Near-Infrared (NIR) region of the atmospheric propagation spectrum is dominated by molecular absorption from H_2O, CO and CO_2. A comparison with recorded spectra enables the identification of relatively strong and isolated CO and CO_2 transitions for unambiguous species detection (Kuang et al., 2002). These transitions have formed the basis of NIR sensors for measurements of CO and CO_2 mole fractions in exhaust gases using extraction-sampling techniques and for non-intrusive measurements of CO_2 in high-temperature combustion environments. Capitalising on the demonstrated potential of Differential Absorption LIDAR (DIAL) (Grant & Hake Jr, 1975; Grant et al., 1974; Schotland, 1974), new airborne DIAL systems will greatly benefit from the advantages offered by powerful, tuneable, compact and low-cost Quantum Cascade Laser (QCL) , enabling large portions of the mid-infrared and far-infrared spectrum (Beck et al., 2002; Faist et al., 1994; Li et al., 2013; McManus et al., 2002; Santoni et al., 2014; Wysocki et al., 2005).

3. Bistatic DIAL Measurement System

As depicted in Fig. 1, the proposed bistatic DIAL measurement system consists of an airborne LIDAR emitter installed on a UA, and a ground-based receiver. The receiver is composed by a target surface of high and diffused reflectance, exhibiting Lambertian behaviour, such as Spectralon™, and a NIR camera mounted on a rail. The UA platform flies pre-determined trajectories based on the required space and time frames of the measurement. The measurement system is based on the Differential Absorption LIDAR (DIAL) technique (Gardi, Sabatini & Wild, 2014). The laser source emits beams at two predefined wavelengths. The first wavelength, λ_{ON}, is selected in correspondence of a major vibrational band of the pollutant molecule (on-absorption line), in a relatively transparent region in the spectrum of all remaining species, and clear from their transition/vibration features. The second wavelength, λ_{OFF}, is selected in proximity of the first, but outside the vibrational band (off-absorption line), so that the difference in cross-sections, $\Delta\psi \triangleq \psi(\lambda_{ON}) - \psi(\lambda_{OFF})$ is maximised. The functional block diagram of the bistatic DIAL measurement system is represented in Fig. 2.

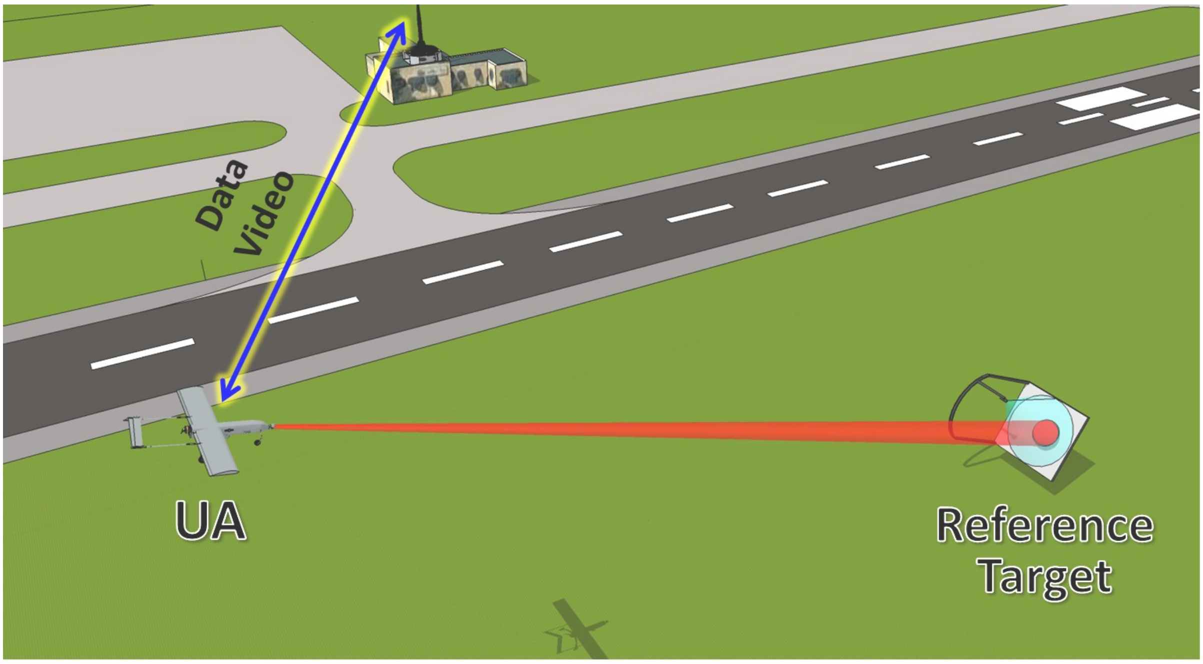

Fig. 1. Conceptual representation of the bistatic DIAL system (not to scale).

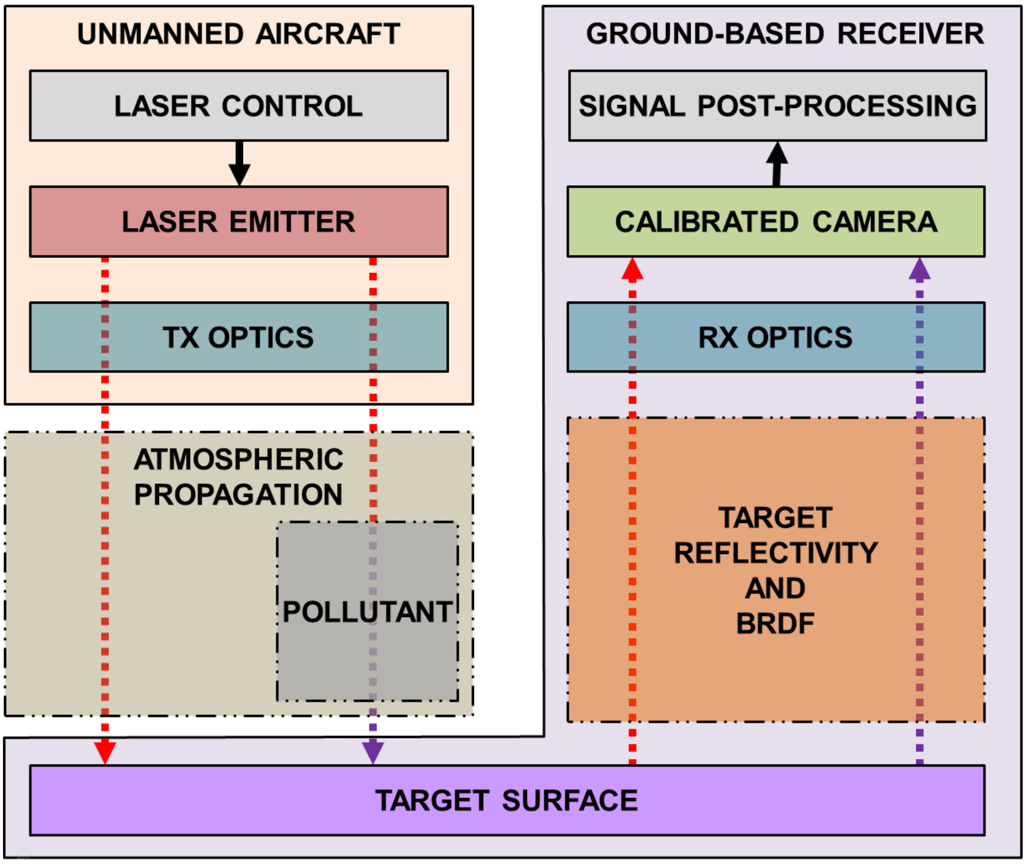

Fig. 2. Functional block diagram of the bistatic DIAL measurement system.

A number of databases and atmospheric Radiative Transfer Model (RTM) codes are available and allow an accurate estimation of the propagation spectrum for the identification of the optimal DIAL wavelengths combination based on the mentioned criteria. For the specific carbon dioxide (CO_2) measurement system implementation, the most suitable absorption wavelength in the NIR spectrum is the centre-line of R-branch at $\lambda_{ON} = 1572.335\ nm$ (Abshire, Ramanathan, et al., 2013; Abshire et al., 2010; Abshire, Riris, et al., 2013; Allan et al., 2008; Amediek et al., 2009; Krainak et al., 2003; Riris et al., 2007).

4. Atmospheric Laser Beam Propagation

The propagation of laser radiation in atmosphere is affected by a number of linear and nonlinear effects. In (Gardi, Sabatini & Ramasamy, 2014) we described the following expression for the peak irradiance I_P, accounting for absorption, scattering, diffraction, jitter, atmospheric turbulence and thermal blooming effects assuming a Gaussian profile of the laser beam at the source and an average focused irradiance (Gebhardt, 1976; Sabatini & Richardson, 2013):

$$I_P(z,\lambda) = \frac{b(z)\ \tau(z,\lambda)\ P(\lambda)}{\pi\left(a_d^2(z,\lambda) + a_j^2(z) + a_t^2(z,\lambda)\right)} \quad (1)$$

where z is the linear coordinate along the beam, λ is the wavelength, $P(\lambda)$ is the transmitted laser power, b is the blooming factor, $\tau(z,\lambda)$ is the transmittance coefficient, which accounts for absorption and scattering associated with all molecular and aerosol species present in the path. The 1/e beam radiuses associated with diffraction, $a_d(z,\lambda)$, beam jitter, $a_j(z)$, and turbulence, $a_t(z,\lambda)$, can be calculated as (Gebhardt, 1976; Sabatini & Richardson, 2010a):

$$a_d(z,\lambda) = \frac{Qz\lambda}{2\pi a_0} \quad (2)$$

$$a_j^2(z) = 2\langle\Theta_x^2\rangle\ z^2 \quad (3)$$

$$a_t(z,\lambda) = \frac{2\ C_N^{6/5} z^{8/5}}{\lambda^{1/5}} \quad (4)$$

where Q is the beam quality factor, a_o is the beam *1/e* radius, $\langle\Theta_x^2\rangle$ is the variance of the single axis jitter angle that is assumed to be equal to $\langle\Theta_y^2\rangle$, and C_N^2 is the refractive index structure constant. An empirical model for the blooming factor $b(z)$, which is the ratio of the bloomed I_B to unbloomed I_{UB} peak irradiance, is:

$$b(z) = \frac{I_B}{I_{UB}} = \frac{1}{1 + 0.0625\ N^2(z)} \quad (5)$$

N is the thermal distortion parameter, calculated as:

$$N(z) = \frac{-n_T\ \alpha_m\ P\ z^2}{\pi\ d_0\ v_0\ c_P\ a_0^3} \cdot \left[\frac{2}{z^2}\int_0^R \frac{a_0}{a(z')}\,dz' \int_0^{z'} \frac{a_0^2\ v_0\ \tau''}{a}\ dz''\right] \quad (6)$$

where v_o is the uniform wind velocity in the weak attenuation limit ($\gamma z \ll 1$), n_T , d_o , and c_p are, respectively, the coefficients of index change with respect to temperature, density, and specific heat at constant pressure. The transmittance coefficient τ depends on the integral effect of absorption and scattering phenomena, both for molecular and aerosol species, on the entire beam length. The expression of Beer's law highlighting such dependences can therefore be written as:

$$\tau(z,\lambda) = e^{-\int_0^z \gamma(z,\lambda)\ dz} = e^{-\int_0^z [\alpha_m(z,\lambda) + \alpha_a(z,\lambda) + \beta_m(z,\lambda) + \beta_a(z,\lambda)]\ dz} \quad (7)$$

where α are the absorption coefficients and β are the scattering coefficients, the subscripts m and a refer respectively to molecular and aerosol contributions. When referring to the integral absorption and scattering due to specific molecular species, it is more appropriate to express the transmittance with the following model:

$$\tau(z,\lambda) = e^{-\int_0^z \gamma(z,\lambda)\ dz} = e^{-\int_0^z \sum_i [\psi_i(\lambda) \cdot n_i(z)]\ dz} \quad (8)$$

where:

$\psi_i(\lambda)$ = cross-section of the i[th] species
n_i = molecular volume density of the i[th] species

From Eq. 8, the fraction between the measured incident laser energy associated with the on-absorption line of pollutant species *P* and the one associated with the off-absorption line, $R_{ON/OFF}$, can be expressed as (Gardi, Sabatini & Wild, 2014):

$$R_{ON/OFF} = \frac{E(\lambda_{ON})}{E(\lambda_{OFF})} = \frac{\tau_{ON}}{\tau_{OFF}} = e^{-[\psi_P(\lambda_{ON})-\psi_P(\lambda_{OFF})]\int_0^D n_P(r)\,dr} \quad (9)$$

where *D* is the total beam length. The total pollutant column density N_P, which is the integral of the molecular volume density on the entire beam, is therefore:

$$N_P = \int_0^D n_P(r)\,dr = \frac{-\ln(R_{ON/OFF})}{\Delta\psi} \quad (10)$$

The average molecular volume concentration of the pollutant on the path, $\tilde{n}_P$, is therefore:

$$\tilde{n}_P = \frac{N_P}{D} = \frac{-\ln(R_{ON/OFF})}{D\cdot\Delta\psi} \quad (11)$$

As evident from Eq. 9 to 11, the bistatic DIAL measurement system neglects most of the parasite phenomena such as atmospheric visibility, particulate, rain and other precipitations, which would have elsewhere introduced a number of additional uncertainties in the system. The parasite effects, in fact, are assumed to equally affect the off-absorption and the on-absorption transmittances. The uncertainty associated with the measurement of the molecular volume concentration, derived from Eq. 11, was derived as (Gardi, Sabatini & Ramasamy, 2014):

$$\sigma_{\tilde{n}_P} = \frac{1}{D\cdot\Delta\psi}\sqrt{\left(\frac{\sigma_{R_{ON/OFF}}}{R_{ON/OFF}}\right)^2 + \left(\frac{\sigma_D \ln R_{ON/OFF}}{D}\right)^2 + \left(\frac{\sigma_{\Delta\psi} \ln R_{ON/OFF}}{\Delta\psi}\right)^2} \quad (12)$$

For a preliminary estimation, we introduced representative errors on the first two quadratic terms in eq. 12, specific to the bistatic DIAL implementation. Errors were introduced on the distance, σ_D, and on the differential energy measurement, which is translated into $\sigma_{R_{ON/OFF}}$ by means of the Bidirectional Reflectance Distribution Function (BRDF) of the target surface (Sabatini & Richardson, 2010a). Assuming a horizontal distance between the UA and the target surface of 1000 m, an UA altitude of 150 m Above Ground Level (AGL), a CO_2 volume density of 300 ppm, and injecting source errors of $\frac{\sigma_{R_{ON/OFF}}}{R_{ON/OFF}} = 3.04\%$ and $\frac{\sigma_D}{D} = 2.47\%$, the relative error in the CO_2 volume density measurement is $\frac{\sigma_{\tilde{n}_P}}{\tilde{n}_P} = 6.77\%$ (Gardi, Sabatini & Ramasamy, 2014). These preliminary estimates, associated with the estimated performance of the calibration technique proposed in (Gardi, Sabatini & Wild, 2014), contribute to supporting the validity of the proposed bistatic DIAL measurement technique for high accuracy sensing of aviation-related pollutant concentrations. Experimental testing will be required to further corroborate these preliminary findings.

5. Model-Based Approach

Analytical expressions of the transmittances were developed for all the atmospheric windows in the infrared spectrum considering the parasite effects of atmospheric visibility, precipitation and fog (Sabatini & Richardson, 2010a). By means of analytical inversion of the transmittance models, and thanks to an accurate sensing of local atmospheric conditions, it is also possible to determine the pollutant concentration without employing differential absorption measurements, by measuring the difference between the actually detected incident energy on the on-absorption line alone, and the model-based prediction for the off-absorption line. Although this technique simplifies the system architecture and potentially enable the adoption of less expensive non-tuneable laser emitters, the resulting error is heavily dependent on the quality and confidence of the measure of all parasite factors such as atmospheric visibility, temperature, pressure, humidity and precipitation. The theoretical model is based on comparison with the available extinction models for the *i*^th^ atmospheric window (Sabatini & Richardson, 2013). By introducing the total condensed water along the laser beam path, *w*, the meteorological visibility, *V*, and the rainfall rate R,the empirically derived atmospheric transmittance values (off-absorption) for the 4th atmospheric window are summarised in Table 1 (Sabatini & Richardson, 2013), where $k_{1,2\ldots6}$ are correction factors experimentally determined as in (Sabatini & Richardson, 2010a). The expressions of Table 1 are valid at mean sea level only. In order to extend the validity of the models, the dependency on altitude h Above Mean Sea Level (AMSL) shall be introduced. A number of empirical relationships for the altitude correction have been experimentally determined for

NIR lasers depending on the grazing angles (Sabatini & Richardson, 2010a). Future research activities will be performed to further characterise the grazing angle dependency for the typical operational configurations of the UA bistatic DIAL measurement system.

Table 1. Empirical expressions for the atmospheric off-absorption transmittance in the 4th atmospheric window.

CONDITION	EMPIRICAL MODEL
$V \geq 6\,km, \quad w \geq 1.1\,mm$	$\tau_{OFF}(z,w,V) \cong \mathrm{k}_1 \cdot 0.6432 \left(\frac{1.1}{w}\right)^{0.222} \cdot e^{-\frac{3.91}{V} z\, 0.3836^{-(0.0057V+1.025)}}$
$V < 6\,km, \quad w \geq 1.1\,mm$	$\tau_{OFF}(z,w,V) \cong \mathrm{k}_2 \cdot 0.6432 \left(\frac{1.1}{w}\right)^{0.222} \cdot e^{-\frac{3.91}{V} z\, 0.3836^{-0.585\sqrt[3]{V}}}$
$V \geq 6\,km, \quad w < 1.1\,mm$	$\tau_{OFF}(z,w,V) \cong \mathrm{k}_3 \cdot e^{-0.422\sqrt{w}-\frac{3.91}{V} z\, 0.3836^{-(0.0057V+1.025)}}$
$V < 6\,km, \quad w < 1.1\,mm$	$\tau_{OFF}(z,w,V) \cong \mathrm{k}_4 \cdot e^{-0.422\sqrt{w}-\frac{3.91}{V} z\, 0.3836^{-0.585\sqrt[3]{V}}}$
rain and $w \geq 1.1\,mm$	$\tau_{OFF}(z,w,R) \cong \mathrm{k}_5 \cdot e^{-0.422\sqrt{w}-0.365\, z\, R^{0.63}}$
rain and $w < 1.1\,mm$	$\tau_{OFF}(z,w,R) \cong \mathrm{k}_6 \cdot 0.6432 \left(\frac{1.1}{w}\right)^{0.222} \cdot e^{-0.365\, z\, R^{0.63}}$

6. Sensor calibration

The photo-camera calibration is an experimental procedure that allows determination of the Integrated Radiance Response Function (AIRF) (Sabatini & Richardson, 2003, 2010b). A highly selective filter (i.e., response centred on the laser wavelength) is used in conjunction with the photo-camera to detect the laser spot energy on the target and to generate a Pixel Intensity Matrix (PIM) in a high resolution greyscale format. The calibration setup is shown in Fig. 3.

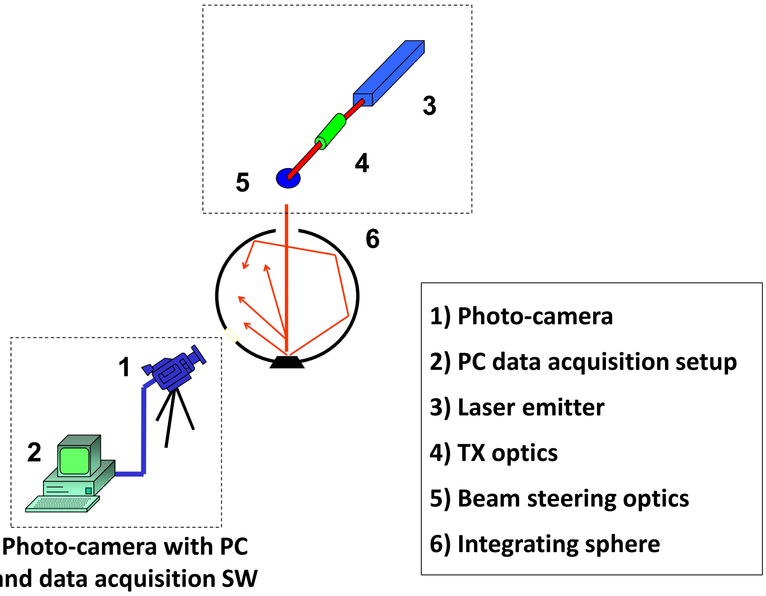

Fig. 3. Layout of the photo-camera calibration.

The response of a single pixel in terms of Analogue Digital Unit (ADU) is:

$$ADU_{i,j} \propto \frac{A}{4 \cdot f_{\#}^{2}+1} \cdot g \cdot i_{time} \cdot \int_{\lambda_1}^{\lambda_2} (\tau_O \cdot \eta_D \cdot E_S)\, \mathrm{d}\lambda \tag{13}$$

where:

$\lambda_{1,2}$	=	limits of the photo-camera spectral band filter
η_D	=	detector quantum efficiency
E_S	=	spectral radiance
τ_O	=	optics transmittance
A	=	pixel area
g	=	read-out electronics gain
$f_{\#}$	=	optics f-number
i_{time}	=	photo-camera integration time

Therefore, the experimental parameters to be controlled during the calibration procedure are the integration time, the optics *f*-number and other settings of the photo-camera (e.g., the gain of the read-out electronics which may be selected by the operator). Fixing these parameters for a certain interval of integral radiance, it is possible to determine the AIRF of the camera by using an extended reference source. The function (calibration curve) so obtained is then used to determine the values of integral radiance for reconstructing the radiant intensity map of the target. Some mathematical models were developed and experimentally validated to calculate the optimal frame rate of the photo-camera (Sabatini & Richardson, 2010a). In particular, photo-cameras are characterised by acquisition frequencies that typically are significantly different from the laser operating PRF. In the bistatic DIAL case, some additional consideration must be given to the alternated wavelengths of different pulses. A conceptual representation of the camera acquisition windows and dark zones in presence of laser pulses of alternating wavelength (different shades of red) is presented in Fig. 4. The parameters describing the train of pulses are the pulse duration (τ), the pulse period (T_P) and the PRF (*f*). Similarly, the camera image acquisition process is defined by the frame period (T_F) and the camera acquisition time (T_A). Generally T_A is inferior to T_F. The difference between T_F and T_A is the so called camera 'dark-time' (T_{dark}).

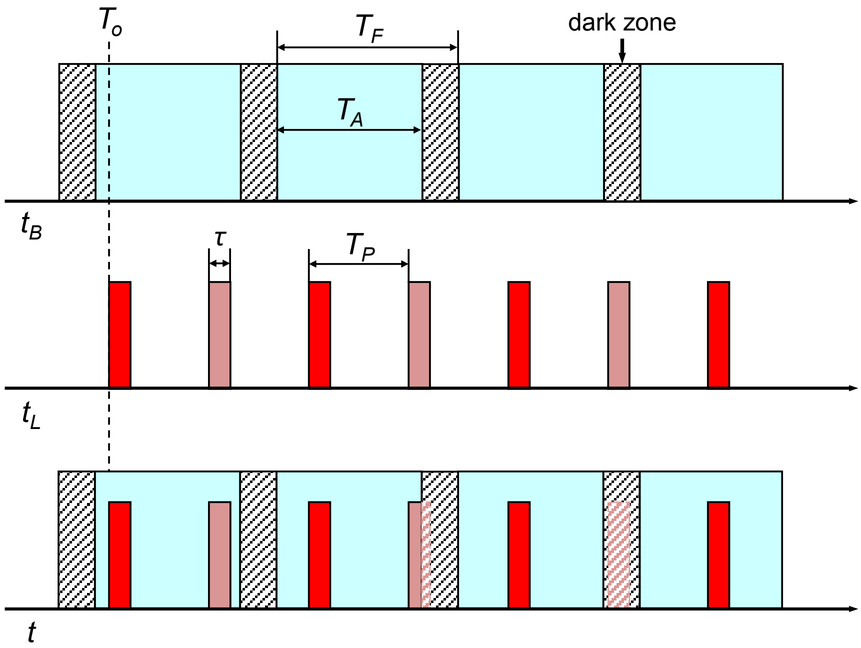

Fig. 4. Photo-camera acquisition sequence and laser pulses.

Good synchronisation is extremely difficult even at low PRF and almost impossible as the PRF increases. Therefore a careful analysis is required in order to determine the optimal frame rate for the camera acquisition as a function of known laser pulse parameters. Since the camera frames are not synchronised with the laser pulses, considering the camera acquisition windows sequence as time base (t_B), the instant of arrival of the first laser pulse (reflected from the target) at the camera (T_o) can be treated as a random variable. Example results of a frame rate optimisation analysis, referred to laser emitters operating at f = 10 Hz and f = 40 kHz are summarised in Fig. 5, where P_{err} is the error probability.

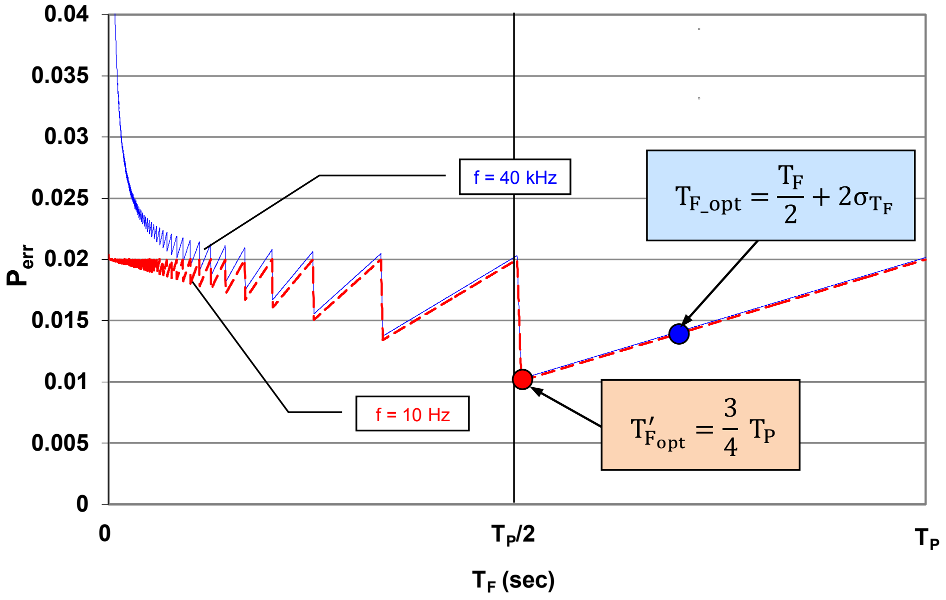

Fig. 50. Results of NIR camera frame rate optimisation analysis

7. Conclusions and Future Work

This paper reviewed the recent research activities focussing on the development of an innovative eye-safe bistatic LIDAR system for the measurement of pollutant concentrations. The specific implementation for carbon dioxide (CO_2) measurement was presented. The Differential Absorption LIDAR (DIAL) technique allows neglecting parasite effects on the measure due to other molecular species and contributes to the overall accuracy and reliability of the proposed technique. The uncertainty analysis for CO_2 column density measurements showed that the proposed technique produces satisfactory results even in degraded meteorological conditions, which are comparable to the more complex and relatively costly techniques currently available. Future research activities will investigate the extension of the system to other families of aviation pollutants such as nitrogen oxides (NO_X), sulphur oxides (SO_X), and Volatile Organic Compounds (VOC), also capitalising on the recent diffusion of powerful tuneable Quantum Cascade Laser (QCL) emitters. The research activities will involve laboratory testing as well as flight testing in various representative conditions. In particular, the development of the airborne component will benefit from the concurrent research activities on UA-based LIDAR systems (Sabatini, Gardi & Ramasamy, 2014; Sabatini, Gardi, Ramasamy, et al., 2014; Sabatini, Gardi & Richardson, 2014). The UA platform will feature Differential GPS-based Time-and-Space-Position-Information (TSPI) systems that were developed for augmented navigation performance of both manned and unmanned aircraft (Sabatini, 1999; Sabatini & Palmerini, 2008) in combination with integrity augmentation systems (Sabatini, Moore, et al., 2012; Sabatini et al., 2013a, 2013b). The experimental flight testing activity will be performed in a suitably developed laser test range in full compliance with the eye-safety requirements (Sabatini, 2014; Sabatini & Richardson, 2003, 2010a).The full potential of the proposed bistatic DIAL measurement system will be exploited through its functional integration in the future Air Traffic Management (ATM) systems (Gardi et al., 2013; Gardi, Sabatini, Ramasamy, et al., 2014; Ramasamy et al., 2014; Ramasamy et al., 2013).

References

Abshire, JB, Ramanathan, A, Riris, H, Mao, J, Allan, GR, Hasselbrack, WE, Weaver, CJ & Browell, EV 2013, 'Airborne measurements of CO2 column concentration and range using a pulsed direct-detection IPDA lidar', *Remote Sensing*, vol. 6, no. 1, pp. 443-69. DOI: 10.3390/rs6010443

Abshire, JB, Riris, H, Allan, GR, Weaver, CJ, Mao, J, Sun, X, Hasselbrack, WE, Kawa, SR & Biraud, S 2010, 'Pulsed airborne lidar measurements of atmospheric CO2 column absorption', *Tellus, Series B: Chemical and Physical Meteorology*, vol. 62, no. 5, pp. 770-83. DOI: 10.1111/j.1600-0889.2010.00502.x

Abshire, JB, Riris, H, Weaver, CJ, Mao, J, Allan, GR, Hasselbrack, WE & Browell, EV 2013, 'Airborne measurements of CO2 column absorption and range using a pulsed direct-detection integrated path differential absorption lidar', *Applied Optics*, vol. 52, no. 19, pp. 4446-61. DOI: 10.1364/AO.52.004446

Allan, GR, Riris, H, Abshire, JB, Sun, X, Wilson, E, Burris, JF & Krainak, MA 2008, 'Laser sounder for active remote sensing measurements of CO2 concentrations', in proceedings of IEEE/AIAA Aerospace Conference 2008 (AC2008), Big Sky, MT, USA, 1-8 March 2008. DOI: 10.1109/AERO.2008.4526387

Amediek, A, Fix, A, Ehret, G, Caron, J & Durand, Y 2009, 'Airborne lidar reflectance measurements at 1.57 µm in support of the A-SCOPE mission for atmospheric CO2', *Atmospheric Measurement Techniques Discussions*, vol. 2, no. 3, pp. 1487-536

Beck, M, Hofstetter, D, Aellen, T, Faist, J, Oesterle, U, Ilegems, M, Gini, E & Melchior, H 2002, 'Continuous wave operation of a mid-infrared semiconductor laser at room temperature', *Science*, vol. 295, no. 5553, pp. 301-5. DOI: 10.1126/science.1066408

Faist, J, Capasso, F, Sivco, DL, Sirtori, C, Hutchinson, AL & Cho, AY 1994, 'Quantum cascade laser', *Science*, vol. 264, no. 5158, pp. 553-6

Gardi, A, Sabatini, R & Ramasamy, S 2014, 'Bistatic LIDAR System for the Characterisation of Aviation-Related Pollutant Column Densities', *Applied Mechanics and Materials*, vol. 629, pp. 257-62. DOI: 10.4028/www.scientific.net/AMM.629.257

Gardi, A, Sabatini, R, Ramasamy, S & de Ridder, K 2013, '4-Dimensional Trajectory Negotiation and Validation System for the Next Generation Air Traffic Management', in proceedings of AIAA Guidance, Navigation, and Control Conference 2013 (GNC 2013), Boston, MA, USA. DOI: 10.2514/6.2013-4893

Gardi, A, Sabatini, R, Ramasamy, S & Kistan, T 2014, 'Real-Time Trajectory Optimisation Models for Next Generation Air Traffic Management Systems', *Applied Mechanics and Materials*, vol. 629, pp. 327-32. DOI: 10.4028/www.scientific.net/AMM.629.327

Gardi, A, Sabatini, R & Wild, G 2014, 'Unmanned aircraft bistatic lidar for CO2 colum density determination', in proceedings of IEEE Metrology for Aerospace (MetroAeroSpace) 2014, Benevento, Italy, 29-30 May 2014. DOI: 10.1109/MetroAeroSpace.2014.6865892

Gebhardt, FG 1976, 'High Power Laser Propagation', *Applied Optics*, vol. 15, no. 6, pp. 1479-93

Grant, WB & Hake Jr, RD 1975, 'Calibrated remote measurements of SO2 and O3 using atmospheric backscatter', *Journal of Applied Physics*, vol. 46, no. 7, pp. 3019-23. DOI: 10.1063/1.321992

Grant, WB, Hake Jr, RD, Liston, EM, Robbins, RC & Proctor Jr, EK 1974, 'Calibrated remote measurement of NO2 using the differential-absorption backscatter technique', *Applied Physics Letters*, vol. 24, no. 11, pp. 550-2. DOI: 10.1063/1.1655049

Janić, M 2007, *The sustainability of air transportation: a quantitative analysis and assessment*, Ashgate Publishing, Ltd.

Krainak, MA, Andrews, AE, Allan, GR, Burris, JF, Riris, H, Sun, X & Abshire, JB 2003, 'Measurements of atmospheric CO2 over a horizontal path using a tunable-diode-laser and erbium-fiber-amplifier at 1572 nm', in proceedings of Conference on Lasers and Electro-Optics 2003 (CLEO '03), Baltimore, MD, USA, 6 June 2003

Kuang, Z, Margolis, J, Toon, G, Crisp, D & Yung, Y 2002, 'Spaceborne measurements of atmospheric CO2 by high-resolution NIR spectrometry of reflected sunlight: An introductory study', *Geophysical Research Letters*, vol. 29, no. 15, pp. 11-1

Li, JS, Chen, W & Fischer, H 2013, 'Quantum cascade laser spectrometry techniques: A new trend in atmospheric chemistry', *Applied Spectroscopy Reviews*, vol. 48, no. 7, pp. 523-59. DOI: 10.1080/05704928.2012.757232

McManus, JB, Nelson Jr, DD, Shorter, J, Zahniser, M, Mueller, A, Bonetti, Y, Beck, M, Hofstetter, D & Faist, J 2002, 'Quantum cascade lasers for open and closed path measurement of atmospheric trace gases', in proceedings of SPIE 4817, Diode Lasers and Applications in Atmospheric Sensing, 47th Annual Meeting, Seattle, WA, USA. DOI: 10.1117/12.452093

Müller, D, Wagner, F, Wandinger, U, Ansmann, A, Wendisch, M, Althausen, D & Von Hoyningen-Huene, W 2000, 'Microphysical particle parameters from extinction and backscatter lidar data by inversion with regularization: Experiment', *Applied Optics*, vol. 39, no. 12, pp. 1879-92

Ramasamy, S, Sabatini, R, Gardi, A & Kistan, T 2014, 'Next Generation Flight Management System for Real-Time Trajectory Based Operations', *Applied Mechanics and Materials*, vol. 629, pp. 344-9. DOI: 10.4028/www.scientific.net/AMM.629.344

Ramasamy, S, Sabatini, R, Gardi, A & Liu, Y 2013, 'Novel flight management system for real-time 4-dimensional trajectory based operations', in proceedings of AIAA Guidance, Navigation, and Control Conference 2013 (GNC 2013), Boston, MA, USA. DOI: 10.2514/6.2013-4763

Riris, H, Abshire, JB, Allan, G, Burris, JF, Chen, J, Kawa, SR, Mao, J, Krainak, M, Stephen, M, Sun, X & Wilson, E 2007, 'A laser sounder for measuring atmospheric trace gases from space', in proceedings of SPIE 6750, Lidar Technologies, Techniques, and Measurements for Atmospheric Remote Sensing III, Florence, Italy. DOI: 10.1117/12.737607

Rodgers, CD 2000, *Inverse methods for atmospheric sounding: Theory and practice*, vol. 2, World scientific Singapore.

Sabatini, R 1999, 'High Precision DGPS and DGPS/INS Positioning for Flight Testing', in *RTO-MP-043 - 6th Saint Petersburg International Conference on Integrated Navigation Systems*, NATO Research and Technology Organization (RTO), Saint Petersburg, Russia, pp. 18-1 to -7.

Sabatini, R 2014, 'Innovative Flight Test Instrumentation and Techniques for Airborne Laser Systems Performance Analysis and Mission Effectiveness Evaluation', in proceedings of IEEE Metrology for Aerospace 2014 (MetroAeroSpace 2014), Benevento, Italy. DOI: 10.1109/MetroAeroSpace.2014.6865886

Sabatini, R, Gardi, A & Ramasamy, S 2014, 'A Laser Obstacle Warning and Avoidance System for Unmanned Aircraft Sense-and-Avoid', *Applied Mechanics and Materials*, vol. 629, pp. 355-60. DOI: 10.4028/www.scientific.net/AMM.629.355

Sabatini, R, Gardi, A, Ramasamy, S & Richardson, MA 2014, 'A Laser Obstacle Warning and Avoidance System for Manned and Unmanned Aircraft', in proceedings of IEEE Metrology for Aerospace (MetroAeroSpace 2014), Benevento, Italy, 29-30 May 2014. DOI: 10.1109/MetroAeroSpace.2014.6865998

Sabatini, R, Gardi, A & Richardson, MA 2014, 'LIDAR Obstacle Warning and Avoidance System for Unmanned Aircraft', *International Journal of Mechanical, Aerospace, Industrial and Mechatronics Engineering*, vol. 8, no. 4, pp. 62-73

Sabatini, R, Moore, T & Hill, C 2012, 'Avionics-based integrity augmentation system for mission- and safety-critical GNSS applications', in proceedings of 25th International Technical Meeting of the Satellite Division of the Institute of Navigation 2012, (ION GNSS 2012), Nashville, TN

Sabatini, R, Moore, T & Hill, C 2013a, 'A new avionics-based GNSS integrity augmentation system: Part 1 - Fundamentals', *Journal of Navigation*, vol. 66, no. 3, pp. 363-84. DOI: 10.1017/S0373463313000027

Sabatini, R, Moore, T & Hill, C 2013b, 'A new avionics-based GNSS integrity augmentation system: Part 2 - Integrity flags', *Journal of Navigation*, vol. 66, no. 4, pp. 501-22. DOI: 10.1017/S0373463313000143

Sabatini, R & Palmerini, GB 2008, *Differential Global Positioning System (DGPS) for Flight Testing, RTO AGARDograph AG-160 Vol. 21*, NATO Science and Technology Organization.

Sabatini, R & Richardson, MA 2003, 'A new approach to eye-safety analysis for airborne laser systems flight test and training operations', *Optics and Laser Technology*, vol. 35, no. 3, pp. 191-8. DOI: 10.1016/S0030-3992(02)00171-8

Sabatini, R & Richardson, MA 2008, 'Innovative methods for planetary atmospheric sounding by lasers', in proceedings of AIAA Space 2008 Conference, San Diego, CA, USA. DOI: 10.2514/6.2008-7670

Sabatini, R & Richardson, MA 2010a, *Airborne Laser Systems Testing and Analysis, RTO AGARDograph AG-300 Vol. 26*, Systems Concepts and Integration Panel (SCI-126), NATO Science and Technology Organization.

Sabatini, R & Richardson, MA 2010b, *RTO AGARDograph AG-300 Vol. 26: Airborne Laser Systems Testing and Analysis*, Systems Concepts and Integration Panel (SCI-126), NATO Science and Technology Organization.

Sabatini, R & Richardson, MA 2013, 'Novel atmospheric extinction measurement techniques for aerospace laser system applications', *Infrared Physics and Technology*, vol. 56, pp. 30-50. DOI: 10.1016/j.infrared.2012.10.002

Sabatini, R, Richardson, MA, Jia, H & Zammit-Mangion, D 2012, 'Airborne laser systems for atmospheric sounding in the near infrared', in proceedings of SPIE 8433, Laser Sources and Applications, Photonics Europe 2012, Brussels, Belgium. DOI: 10.1117/12.915718

Santoni, GW, Daube, BC, Kort, EA, Jiménez, R, Park, S, Pittman, JV, Gottlieb, E, Xiang, B, Zahniser, MS, Nelson, DD, McManus, JB, Peischl, J, Ryerson, TB, Holloway, JS, Andrews, AE, Sweeney, C, Hall, B, Hintsa, EJ, Moore, FL, Elkins, JW, Hurst, DF, Stephens, BB, Bent, J & Wofsy, SC 2014, 'Evaluation of the airborne quantum cascade laser spectrometer (QCLS) measurements of the carbon and greenhouse gas suite-CO2, CH4, N2O, and CO-during the CalNex and HIPPO campaigns', *Atmospheric Measurement Techniques*, vol. 7, pp. 1509-26. DOI: 10.5194/amt-7-1509-2014

Schotland, RM 1974, 'Errors in the lidar measurement of atmospheric gases by differential absorption', *Journal of Applied Meteorology*, vol. 13, no. 1, pp. 71-7

Veselovskii, I, Kolgotin, A, Griaznov, V, Müller, D, Franke, K & Whiteman, DN 2004, 'Inversion of multiwavelength Raman lidar data for retrieval of bimodal aerosol size distribution', *Applied Optics*, vol. 43, no. 5, pp. 1180-95. DOI: 10.1029/2003JD003538

Wysocki, G, Curl, RF, Tittel, FK, Maulini, R, Bulliard, JM & Faist, J 2005, 'Widely tunable mode-hop free external cavity quantum cascade laser for high resolution spectroscopic applications', *Applied Physics B: Lasers and Optics*, vol. 81, no. 6, pp. 769-77. DOI: 10.1007/s00340-005-1965-4